

***Tupaia* OASL1 Promotes Cellular Antiviral Immune Responses by Recruiting MDA5 to MAVS**

This information is current as of December 28, 2020.

Yu-Lin Yao, Dandan Yu, Ling Xu, Tianle Gu, Yu Li, Xiao Zheng, Rui Bi and Yong-Gang Yao

*J Immunol* 2020; 205:3419-3428; Prepublished online 13 November 2020;

doi: 10.4049/jimmunol.2000740

<http://www.jimmunol.org/content/205/12/3419>

**Supplementary Material** <http://www.jimmunol.org/content/suppl/2020/11/12/jimmunol.2000740.DCSupplemental>

**References** This article **cites 48 articles**, 8 of which you can access for free at: <http://www.jimmunol.org/content/205/12/3419.full#ref-list-1>

**Why *The JI*?** [Submit online.](#)

- **Rapid Reviews!** 30 days\* from submission to initial decision
- **No Triage!** Every submission reviewed by practicing scientists
- **Fast Publication!** 4 weeks from acceptance to publication

\*average

**Subscription** Information about subscribing to *The Journal of Immunology* is online at: <http://jimmunol.org/subscription>

**Permissions** Submit copyright permission requests at: <http://www.aai.org/About/Publications/JI/copyright.html>

**Email Alerts** Receive free email-alerts when new articles cite this article. Sign up at: <http://jimmunol.org/alerts>

# *Tupaia* OASL1 Promotes Cellular Antiviral Immune Responses by Recruiting MDA5 to MAVS

Yu-Lin Yao,<sup>\*,†,‡</sup> Dandan Yu,<sup>\*,†,‡</sup> Ling Xu,<sup>\*,†</sup> Tianle Gu,<sup>\*,†,‡</sup> Yu Li,<sup>\*,†,‡</sup> Xiao Zheng,<sup>\*,†,§</sup> Rui Bi,<sup>\*,†,‡</sup> and Yong-Gang Yao<sup>\*,†,‡,¶,||</sup>

**Melanoma differentiation-associated gene 5 (MDA5) is a key cytoplasmic dsRNA sensor. Upon binding to invading viral RNA, activated MDA5 is recruited to mitochondria and interacts with mitochondrial antiviral signaling gene (MAVS) to initiate innate antiviral immune responses. The elegant regulation of this process remains elusive. In this study, using the Chinese tree shrew (*Tupaia belangeri chinensis*), which is genetically close to primates, we identified the *Tupaia* oligoadenylate synthetases-like 1 (tOASL1) as a positive regulator of the *Tupaia* MDA5 (tMDA5) and *Tupaia* MAVS (tMAVS)-mediated IFN signaling. Overexpression of tOASL1 significantly potentiated the RNA virus-triggered induction of the type I IFNs and downstream antiviral genes. Conversely, knockdown of tOASL1 had an impaired antiviral immune response. Mechanistically, tOASL1 was associated with mitochondria and directly interacted with tMDA5 and tMAVS. Upon RNA virus infection, tOASL1 enhanced the interaction between tMDA5 and tMAVS via its OAS and UBL domains. Our results revealed a novel mechanism by which tOASL1 contributes to host antiviral responses via enhancing tMDA5 and tMAVS interaction. *The Journal of Immunology*, 2020, 205: 3419–3428.**

**T**he innate immune system provides the critical first line of host defense against pathogen invasions via recognition of pathogen-associated molecular patterns aided by pattern recognition receptors, which initiate a series of signaling cascades leading to the induction of the type I IFN and proinflammatory cytokines (1, 2). Viral RNAs derived from the viral

genome or its replication intermediates are mainly recognized by retinoic acid inducible gene I (RIG-I)-like receptors (RLRs) including RIG-I, melanoma differentiation-associated gene 5 (MDA5), and laboratory of genetics and physiology 2 (LGP2) (3, 4). RIG-I and MDA5 contain two caspase activation and recruitment domains (CARDs), a helicase domain, and a C-terminal domain (CTD), and recognize different types of RNA viruses (3, 4). Following ligand binding, RIG-I and MDA5 are recruited to the mitochondrion-associated membrane where they bind to mitochondrial antiviral signaling gene [MAVS (5), also named as IPS-1 (6), Cardif (7) or VISA (8)] via homotypic CARD interaction and promote a massive MAVS prion-like fiber formation (9, 10). Subsequently, MAVS recruited downstream antiviral kinases, such as TRAF3, TBK1/IKK $\epsilon$ , and IKK $\alpha$ / $\beta$ , which further phosphorylate the transcription factors IRF3 and NF- $\kappa$ B to induce the production of type I IFNs. The IFNs trigger the JAK/STAT signaling pathway to increase the expression of hundreds of IFN-stimulated genes (ISGs) and eventually help the host cells to defend from invading viruses (1, 11). In contrast to RIG-I and MDA5, the LGP2 lacks the CARDs and regulates the RLR signaling in response to certain viruses (12–14). To invoke a proper antiviral immune response, signaling proteins involved in these cascades were precisely regulated by immune regulators. Negative regulators dampen innate immune activation and inflammation to avoid additional tissue damage, whereas rapid and robust induction of IFN aided by positive regulators is critical for effective clearance of invading viruses (15).

The 2'-5'-oligoadenylate synthetases (OAS) family proteins are composed of OAS1, OAS2, OAS3, and OAS-like (OASL). All OAS members are characterized by their highly conserved N-terminal OAS domain and play a critical role in blocking viral infections (16, 17). Among them, OAS1, OAS2 and OAS3, possess the 2'-5' oligoadenylates synthetase activity and exert antiviral activity via the canonical RNase L-dependent pathway (18). The OASL is devoid of enzyme activity to synthesize 2'-5' oligoadenylates and exerts its antiviral activity as a multifaceted immune regulator (19). In human beings, the OASL counteracts the RNA virus infections by interacting and enhancing RIG-I

\*Key Laboratory of Animal Models and Human Disease Mechanisms of the Chinese Academy of Sciences and Yunnan Province, Kunming Institute of Zoology, Chinese Academy of Sciences, Kunming, Yunnan 650223, China; <sup>†</sup>Kunming Institute of Zoology – Chinese University of Hong Kong Joint Laboratory of Bioresources and Molecular Research in Common Diseases, Kunming Institute of Zoology, Chinese Academy of Sciences, Kunming, Yunnan 650223, China; <sup>‡</sup>Kunming College of Life Science, University of Chinese Academy of Sciences, Kunming, Yunnan 650204, China; <sup>§</sup>School of Life Sciences, Division of Life Sciences and Medicine, University of Science and Technology of China, Hefei, Anhui 230026, China; <sup>¶</sup>National Resource Center for Non-Human Primates, Kunming Institute of Zoology, Chinese Academy of Sciences, Kunming, Yunnan 650107, China; and <sup>||</sup>Primate Facility, National Research Facility for Phenotypic and Genetic Analysis of Model Animals, Kunming Institute of Zoology, Chinese Academy of Sciences, Kunming, Yunnan 650107, China

ORCIDs: 0000-0002-7309-4250 (X.Z.); 0000-0002-2955-0693 (Y.-G.Y.).

Received for publication June 23, 2020. Accepted for publication October 15, 2020.

This work was supported by the National Natural Science Foundation of China (U1902215 and U1402224 [to Y.-G.Y.]), the West Light Foundation of the Chinese Academy of Sciences (xbzg-zdsys-201909 [to Y.-G.Y.]), and the Yunnan Provincial Natural Science Foundation (2018FB046 and 202001AS070023 [to D.Y.]).

Address correspondence and reprint requests to Dr. Yong-Gang Yao, Kunming Institute of Zoology, Chinese Academy of Sciences, 21 Qingsong Road, Kunming, Yunnan 650204, China. E-mail address: yaoyg@mail.kiz.ac.cn

The online version of this article contains supplemental material.

Abbreviations used in this article: CARD, caspase activation and recruitment domain; CAS, Chinese Academy of Sciences; CTD, C-terminal domain; EMCV, encephalomyocarditis virus; F, forward; hMAVS, human MAVS; hMDA5, human MDA5; hOASL, human OASL; ISD, IFN stimulatory DNA; ISG, IFN-stimulated gene; ISRE, IFN-stimulated response element; KIZ, Kunming Institute of Zoology; KO, knock-out; LGP2, laboratory of genetics and physiology 2; MAVS, mitochondrial antiviral signaling gene; MDA5, melanoma differentiation-associated gene 5; MOI, multiplicity of infection; NDV, Newcastle disease virus; OAS, oligoadenylate synthetase; OASL, OAS-like; poly I:C H, high m.w. poly I:C; RIG-I, retinoic acid inducible gene I; RLR, RIG-I-like receptor; RT-qPCR, quantitative real-time PCR; SeV, Sendai virus; sgRNA, small guide RNA; siNC, small interfering negative control; siRNA, small interfering RNA; sitOASL, small interfering tOASL; tMAVS, *Tupaia* MAVS; tMDA5, *Tupaia* MDA5; tOASL1, *Tupaia* OASL1; TSPRC, tree shrew primary renal cell; VSV, vesicular stomatitis virus; WT, wild-type.

Copyright © 2020 by The American Association of Immunologists, Inc. 0022-1767/20/\$37.50

activation (20). However, the OASL has an inhibitory effect on cGAS activity to reduce IFN induction during DNA virus infection (21). Unlike human, mouse Oasl1 specifically binds to IRF7 5' untranslated region and inhibits the translation of IRF7 mRNA, thus negatively regulating the antiviral innate immunity regardless of DNA and RNA virus infections (22).

We recently characterized the OASs (including tOAS1, tOAS2, *Tupaia* OASL [tOASL] 1, and tOASL2) of the Chinese tree shrew (*Tupaia belangeri chinensis*) (23), which is a small mammal genetically closer to primates (24, 25) and has been used as a good model for studying infectious diseases (26–30) and other diseases (31–33). We found that the antiviral activities of tOAS1 and tOAS2 were dependent on the canonical RNase L pathway, whereas those of tOASL1 and tOASL2 were independent on the RNase L pathway (23). In this study, we aimed to test whether tOASs block viral replications through regulating antiviral innate immune responses. We identified tOASL1 as a positive regulator in RNA virus-induced production of type I IFN mediated by *Tupaia* MDA5 (tMDA5) and *Tupaia* MAVS (tMAVS).

## Materials and Methods

### Ethics statement

The healthy adult Chinese tree shrews ( $n = 10$ ) were introduced from the experimental animal core facility of the Kunming Institute of Zoology (KIZ), Chinese Academy of Sciences (CAS). After euthanasia, we isolated tree shrew primary renal cells (TSPRCs) according to the method of enzyme-assisted dissection, as described in our previous study (34). All experimental procedures were performed with the approval of the Institutional Animal Care and Use Committee of the KIZ (Approval No.: SYDW20110315001).

### Cells, viruses, ligands, and plasmids

Vero, HEK293T, and HeLa cells were introduced from Kunming Cell Bank, KIZ, CAS. Cells were cultured at 37°C in 5% CO<sub>2</sub> with DMEM (11965-092, DMEM; Life Technologies-BRL) supplemented with 10% FBS (10099-141, FBS; Life Technologies-BRL) and 1× penicillin/streptomycin (10378016; Life Technologies-BRL). DNA virus (HSV-1) and RNA viruses (including Sendai virus [SeV], encephalomyocarditis virus [EMCV], Newcastle disease virus [NDV], and vesicular stomatitis virus [VSV]) were taken from our previous study (34). High m.w. poly I:C (poly I:C H) (catalog no. tlr-picl), poly dA:dT (catalog no. tlr-patn), and IFN stimulatory DNA (ISD) (catalog no. tlr-isdn) were from InvivoGen.

Expression vectors for tOAS1, tOAS2, tOASL1, tOASL2, tMAVS, tMDA5, and *Tupaia* LGP2 were taken from our previous studies (23, 34, 35). The Myc-tagged tOASL1 was subcloned into pCS2-N-myc with BspEI and SacI. Expression vector for tTBK1 was generated using specific primers and was cloned into pCMV-3Tag-8 vectors (Supplemental Table I). The tree shrew IFNβ1 promoter luciferase reporter (IFN-β-Luc; pGL3-tIFN-β-promoter), ISRE-Luc (219092, ISRE *cis*-reporter; Stratagene) and NF-κB-Luc (631912, pNFκB-TA-Luc; Clontech Laboratories), and pRL-SV40-*Renilla* (as an internal control; Promega) were from our previous studies (34, 35). We created pCMV-3Tag-8 and pCMV-HA expression vectors for different domains of tOASL1 (tOASL1-OAS and tOASL1-UBL), tMDA5 (tMDA5-CARD, tMDA5-Helicase, and tMDA5-CTD), and tMAVS (tMAVS-CARD, tMAVS pattern recognition receptors, and tMAVS-TM) (Supplemental Table I). All constructs were confirmed by direct sequencing.

### Abs

We used the following primary Abs: mouse monoclonal anti-FLAG (M20008; Abmart), mouse monoclonal anti-HA (3724; Cell Signal Technology), mouse anti-c-Myc (9E11) (MA1-16637; Life Technologies), rabbit monoclonal anti-FLAG (14973; Cell Signal Technology), mouse monoclonal anti-β-actin (E1C602-2; EnoGene), mouse monoclonal anti-GAPDH (E12-052-4; EnoGene), rabbit monoclonal anti-TBK1 (3504; Cell Signal Technology), rabbit monoclonal anti-phospho-TBK1 (Ser172) (5483; Cell Signal Technology), rabbit monoclonal anti-IRF3 (4302; Cell Signal Technology), and rabbit monoclonal anti-phospho-IRF3 (Ser396) (4947; Cell Signal Technology). The NF-κB pathway sample kit (9936; Cell Signal Technology), which contains Abs against phospho-p65 (Ser536), p65, phospho-IKKα/β (Ser176/180), IKKα/β, phospho-IκBα

(Ser32), and IκBα, was used to test the activation of the NF-κB signaling. We used the following secondary Abs: peroxidase-conjugated anti-mouse Ab (474-1806; KPL), peroxidase-conjugated anti-rabbit Ab (074-1506; KPL), Alexa Fluor 594-conjugated anti-rabbit IgG (A21207; Invitrogen), and Alexa Fluor 488-conjugated anti-mouse IgG (A21202; Invitrogen).

### Generation of tOASL1 knockout cell

We used the CRISPR-Cas9 system (36) to knock out the *tOASL1* gene in the TSR6 cell line that was established in our previous study (37). Briefly, small guide RNAs (sgRNAs) (tOASL1-sgRNA-forward [F]: 5'-CACCGTCGCTTTCCCTCACGGT-3'/tOASL1-sgRNA-reverse: 5'-AAACAACCGTGAGTGGAAAGACGAC-3') targeting *tOASL1* were annealed and cloned into the pX330-T7 vector (a kind gift from Dr. P. Zheng, KIZ) expressing mCherry. The TSR6 cells were transfected with the pX330-T7 vector carrying the sgRNAs by using Lipofectamine 3000 (L3000008; Invitrogen). The transfected cells expressing mCherry were sorted by flow cytometry and cultured for 48 h. Single cells were manually picked with a mouth pipette for expansion for 3 wk. We used AxyPrep Multisource Genomic DNA Miniprep Kit (26817KC1; Axygen) to extract genomic DNA of single TSR6 cells with potential knockout (KO) of tOASL1. The gene region spanning the sgRNA targeting sites was amplified by using primer pair tOASL1-sgRNA-Fc: 5'-AGGTGCTGGACTCTGTGAC-3'/tOASL1-sgRNA-Rc: 5'-AGGTGCTGGACTCTGTGAC-3'. The PCR products were sequenced by using primer tOASL1-sgRNA-Fc to screen for mutation(s). We were able to pick up a cell clone with a deletion of 14 bp (c.66\_79del) that disrupts the translation of tOASL1 protein. The KO of endogenous tOASL1 protein was further validated by Western blot.

### RNA interference and transfection

The small interfering RNAs (siRNAs) targeting *tOASL1* and small interfering negative controls (siNC) were synthesized by RiboBio (Guangzhou, China). We designed three siRNAs targeting the *tOASL1* gene: small interfering tOASL (sitOASL) 1-1, 5'-GCACTACACCTTCCAACAT-3'; sitOASL1-2, 5'-CCTTACGAGTCCATAAAGA-3'; and sitOASL1-3, 5'-ACACTACAGCATCCAAGAT-3'. Transfection of siRNA into TSPRCs using Lipofectamine 3000 was performed according to manufacturer's instructions, as described in our previous study (38). The knockdown efficiency of siRNAs was evaluated at the mRNA and protein levels.

### RNA extraction and quantitative real-time PCR

Total RNA was extracted from TSPRCs using the RNAsimple Total RNA Kit (DP419; TIANGEN) according to the manufacturer's instruction. As described in our previous studies (23, 35, 39), the quality of total RNA was measured on a biophotometer (Eppendorf). About 2 μg total RNA (with an A260/A280 ratio of 1.8–2.0) was used to synthesize cDNA by using oligo-dT<sub>18</sub> primer and Moloney murine leukemia virus reverse transcriptase (M1701; Promega). For detection of the viral RNA, we used a virus-specific primer (SeV R15360: 5'-ACCAGACAAGAGTTTAAAGATATG-3') to transcribe the SeV RNA and used a primer pair SeV-F15160: 5'-TGTTCCGGGGCCAGGCAAAAT-3'/SeV-R15247: 5'-GTTCTGCACGATAGGGACTA-3' for quantitative real-time PCR (RT-qPCR). For quantification of EMCV RNA, we used a specific primer for the L antisense (5'-GGCGTCATGGTGGCGAATAAGCGCAGCTCTCACCTTTGA-3') for the transcription and used EMCV common F: 5'-AATAAAT-CATAAGGCCGTCATGGTGGCGAATAA-3'/L reverse primer: 5'-AATAAATCATAATCGAAAACGACTTCCATGTCT-3' for RT-qPCR. For detection of NDV RNA, we used a specific primer (NDV R15168: 5'-ACCAAAACAAGATTTGGTGAATGAC-3') to transcribe the NDV RNA and used primer pair NDV-F15160: 5'-CTTATTACCCCTTACAATC-3'/NDV-R15247: 5'-CTGAGACCCAGTATTGTGAC-3' for RT-qPCR. For detection of HSV-1 RNA, we used HSV-1-F: 5'-TGGGACACATGCCTTCTTGG-3'/HSV-1-R15247: 5'-ACCCTTAGTCA-GACTCTGTACTTACCC-3' for RT-qPCR.

In brief, RT-qPCR was conducted using iTaq Universal SYBR Green Supermix (172-5125; Bio-Rad Laboratories) with gene-specific primer pairs (Supplemental Table I) on a CFX Connect Real-Time PCR Detection System (Bio-Rad Laboratories). The thermal cycling protocol was one cycle at 95°C for 1 min, 40 cycles of 95°C for 15 s, and 55°C for 15 s. The tree shrew β-actin transcript was used for the normalization of the target gene (35).

### Western blotting

We followed the procedures for Western blotting and immunoprecipitation in our previous studies (23, 34). In brief, TSPRCs and HEK293T cells were transfected with the indicated expression vectors and/or *tOASL1* siRNAs

for 48 h using Lipofectamine 3000. Cells were then harvested and lysed in RIPA lysis buffer (P0013; Beyotime Institute of Biotechnology) on ice. Protein concentration was determined by using the BCA protein assay kit (P0012; Beyotime Institute of Biotechnology). Equal amount (20  $\mu$ g) of cellular protein for each sample was used for Western blotting. Electrophoresis was performed using 12% SDS-PAGE. Proteins were transferred onto polyvinylidene fluoride membranes (IPVH00010; Roche Diagnostics) using the standard procedure. After having blocking in 5% nonfat dry milk dissolved in TBS (#9997; Cell Signaling Technology) containing 0.1% Tween 20 (TBST [0.1%, P1379; Sigma]) at room temperature for 2 h, the membranes were incubated with the respective Abs against FLAG (1:5000), HA (1:5000), Myc (1:5000), OASL (1:1000), IRF3 (1:1000), phospho-IRF3 (Ser396) (1:1000), TBK1 (1:1000), phospho-TBK1 (Ser172) (1:1000), p65 (1:1000), phospho-p65 (Ser536) (1:1000), phospho-IKK $\alpha$ / $\beta$  (Ser176/180) (1:1000), IKK $\alpha$ / $\beta$  (1:1000), phospho-I $\kappa$ B $\alpha$  (Ser32) (1:1000), I $\kappa$ B $\alpha$  (1:1000), GAPDH (1:10,000), or  $\beta$ -actin (1:10,000) overnight at 4°C. The membranes were washed three times (5 min each time) with TBST and were incubated with anti-mouse or anti-rabbit secondary Ab (1:10,000; KPL), dependent on the primary Ab, for 1 h at room temperature. After washing, the protein bands were visualized using the ECL reagents (WBKLS0500; MilliporeSigma).

#### Coimmunoprecipitation assay

Cells were lysed in RIPA lysis buffer on ice for 1 h, followed by a centrifuge at 12,000  $\times$  g for 10 min at 4°C. Appropriate Abs were incubated with protein G agarose beads (15920010; Life Technologies) to form a complex for 2 h at room temperature. Then, the protein G agarose bead-conjugated Abs were mixed with the cell lysates to form the protein complex overnight at 4°C. After four washes with the RIPA lysis buffer, the immunoprecipitates were resuspended in loading sample buffer and were analyzed by immunoblot analysis.

#### Luciferase reporter assay

TSPRCs were seeded in 24-well plates at a density of  $1 \times 10^4$  cells and cultured overnight. Cells were transiently transfected with 0.1  $\mu$ g of the luciferase reporter vector, 0.01  $\mu$ g pRL-SV40-*Renilla*, together with the indicated amount of empty vector or expression vector by using XtremeGENE HP DNA Transfection Reagent (06366236001; Roche). After transfection for 36 h, cells were left untreated or infected with NDV (multiplicity of infection [MOI] = 1) or HSV-1 (MOI = 1) for 12 h. Cells were harvested for luciferase activity using the Dual-Luciferase Reporter Assay System (E1960; Promega) on an Infinite M1000 Pro multimode microplate reader (30064852; Tecan).

#### Immunofluorescence analysis

TSPRCs were seeded on glass coverslips and transfected with the indicated expression vectors for 36 h, and then cells were left uninfected or infected with NDV (MOI = 1) for the indicated times. After three washes with PBS, cells were fixed with 300  $\mu$ l 4% paraformaldehyde for 15 min at 37°C, followed by a permeabilized procedure using 0.1% Triton X-100 (Sigma-Aldrich) for 15 min at room temperature. Cells were then incubated with mouse anti-FLAG (1:500), rabbit anti-FLAG (1:500), and mouse anti-HA (1:500) overnight at 4°C. After washing with PBS three times, cells were incubated with the indicated secondary Ab (1:500) at room temperature for 2 h. Cell nuclei were stained with 1  $\mu$ g/ml DAPI (10236276001; Roche Diagnostics). The slides were analyzed using an Olympus FluoView 1000 confocal microscope (Olympus).

#### Mitochondrion isolation

Crude mitochondrion preparations were isolated by using the Mitochondria Crude Isolation Kit (Beyotime Institute of Biotechnology), as described in our previous studies (39). We used the indicated amounts of proteinase K to treat crude mitochondria (~40  $\mu$ g) for 30 min on ice, followed by a treatment with 1 mM PMSF (Sigma-Aldrich) to stop proteinase K activity. Protein denaturation was performed at 95°C for 5 min in NaDodSO<sub>4</sub> loading buffer (Beyotime Institute of Biotechnology), followed by the Western blot assay.

#### VSV plaque assay

We followed the procedure described in our recent study for the VSV plaque assay (38). Briefly, Vero cells were seeded in six-well plates and were infected with VSV supernatants serially diluted (10-fold) in serum-free DMEM. The supernatant was discarded after 1 h postinfection, and 1% low melting-point agarose with growth medium (2 ml/well) was overlaid on the infected cells. At 3 d postinfection, the overlaid agarose was

discarded, and cells were fixed with 4% formaldehyde for 20 min. Cells were further stained with 0.2% crystal violet (Beyotime Institute of Biotechnology) at room temperature for 10 min. The PFU per sample unit volume (PFU/ml) was determined by counting the number of plaques in each well.

#### Statistical analysis

Comparison of the mRNA levels between different groups was analyzed by using the GraphPad software (GraphPad Software) with two-tailed unpaired Student *t* test. Data were presented as mean  $\pm$  SD. A *p* value <0.05 was considered to be statistically significant.

## Results

### *tOASL1* positively regulated the RNA virus-triggered type I IFN signaling

To determine the potential roles of tOAS family members in regulating antiviral signaling, we first performed a functional screening using the IFN- $\beta$  promoter reporter in TSPRCs overexpressing tOAS members. We found that overexpression of tOASL1 significantly enhanced the IFN- $\beta$  promoter activation induced by an RNA virus-NDV but not by a DNA virus-HSV-1 infection (Fig. 1A). The potentiated effect of tOASL1 overexpression on type I IFN signaling upon RNA virus infection, as demonstrated by increased *tIFNB1* mRNA expression, could be well reproduced by challenging with various RNA viruses including SeV, EMCV, NDV, and dsRNA analogue poly I:C H (Fig. 1B, left). tOASL1 overexpression reduced the viral mRNA levels of SeV, EMCV, and NDV (Fig. 1B, right). Consistent with the pattern of Fig. 1A, tOASL1 overexpression had no obvious change on *tIFNB1* mRNA expression in TSPRCs stimulated by HSV-1 and DNA ligands, including poly dA:dT and ISD (Fig. 1B, left), although a lower level of HSV-1 viral RNA was found in TSPRCs overexpressing tOASL1 relative to the empty vector group (Fig. 1B, right). Note that the inhibitory effect of tOASL1 overexpression on HSV-1 viral RNA level was much inferior to those of the viral levels of SeV, EMCV, and NDV (Fig. 1B, right). These results indicated that tOASL1 was actively involved in RNA virus-induced type I IFN signaling. As NDV infection had the best stimulation effect in TSPRCs, we used this virus for stimulation in the subsequent assays unless otherwise stated. Concordantly, tOASL1 overexpression could activate the NDV-triggered IFN- $\beta$  promoter activity in a dose-dependent manner (Fig. 1C). Because IFN- $\beta$  promoter activation is driven by IFN-stimulated response element (ISRE) and NF- $\kappa$ B, we next tested the activation of ISRE and NF- $\kappa$ B promoters in the presence of tOASL1 overexpression and NDV infection. Overexpression of tOASL1 significantly potentiated NDV-induced ISRE and NF- $\kappa$ B activations (Fig. 1D) and enhanced mRNA expression of *tIFNB1* and its downstream genes including *tISG54*, *tISG56*, and *tMx1* (Fig. 1E). Consistently, tOASL1 overexpression increased phosphorylation of TBK1, IRF3, p65, IKK $\alpha$ / $\beta$ , and I $\kappa$ B $\alpha$  upon NDV infection in a time-dependent manner (Fig. 1F). These results demonstrated that tOASL1 activated the IRF3 and NF- $\kappa$ B signaling and positively regulated the antiviral immune responses.

### Endogenous tOASL1 was critically required for antiviral immune responses to RNA virus

To characterize the roles of tOASL1 in antiviral responses, we performed knockdown assays using siRNAs targeting *tOASL1* to reduce endogenous tOASL1 expression. Among the three *tOASL1* siRNAs, sitOASL1-1 exhibited the highest knockdown efficiency, whereas sitOASL1-3 had no obvious inhibitory effect on tOASL1 expression (Fig. 2A). We used sitOASL1-1 for the subsequent experiments. Consistent with the upregulation effect of tOASL1 (Fig. 1C, 1D), knockdown of tOASL1 significantly

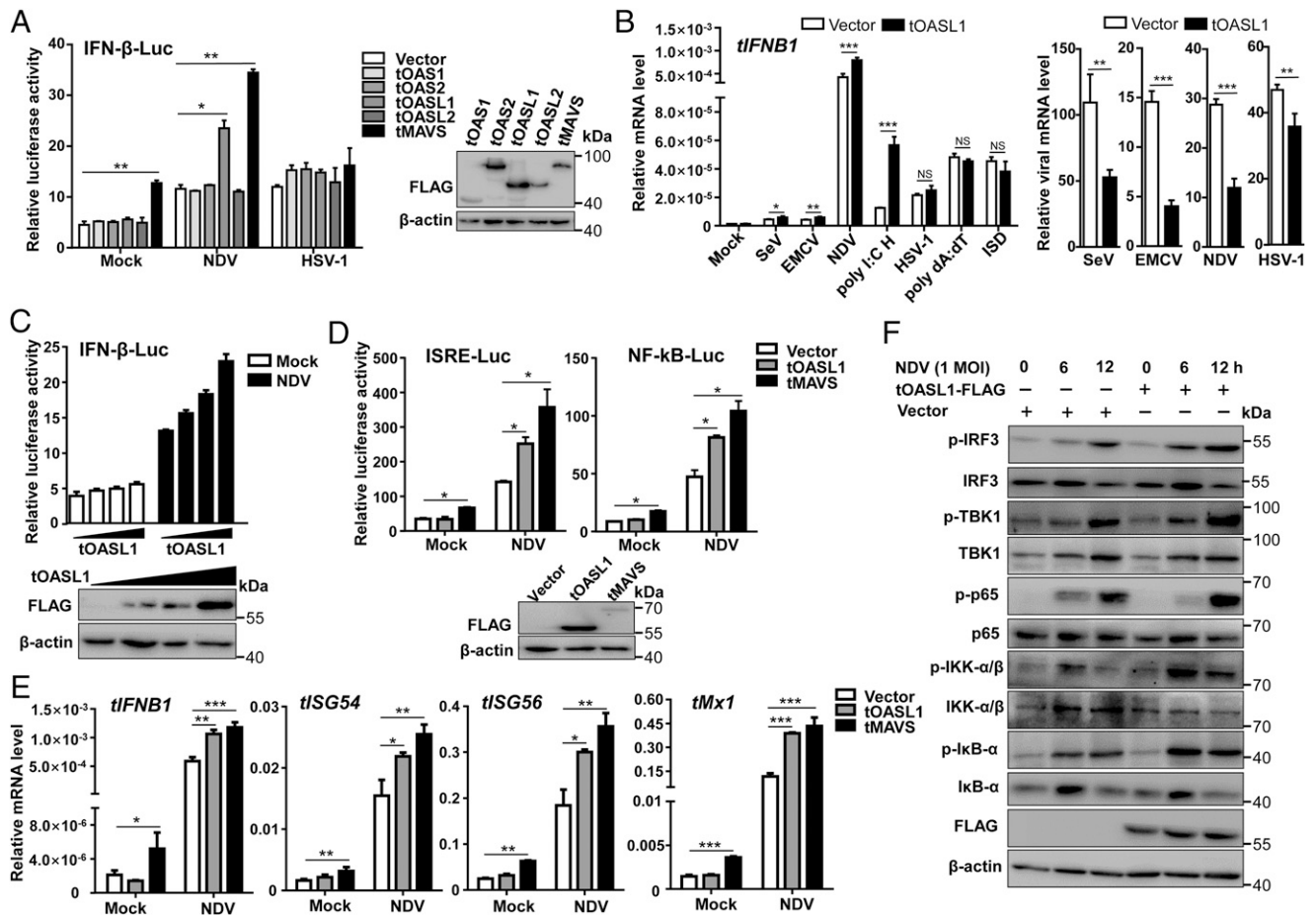


**FIGURE 1.** The tOASL1 is a positive regulator of the antiviral signaling to counteract RNA virus infection. **(A)** Effects of overexpressed tOAS family members (tOAS1, tOAS2, tOASL1, and tOASL2) on IFN-β-Luc reporter activation upon NDV and HSV-1 infection. Left, IFN-β-Luc reporter luciferase activity; right, Western blot showing successful overexpression of the indicated proteins. TSPRCs ( $1 \times 10^5$ ) were cotransfected with the indicated expression vector (400 ng), IFN-β-Luc reporter vector (100 ng), and TK (10 ng, as an inner control) for 36 h, followed by infection with or without NDV (MOI = 1) or HSV-1 (MOI = 1) for 12 h before the harvest. **(B)** Upregulation of the *tIFNB1* mRNA level by overexpressed tOASL1 in TSPRCs infected with RNA virus infection. Left, Cells ( $1 \times 10^5$ ) were transfected with empty vector (Vector) and tOASL1 (each 500 ng) for 36 h, followed by infection with SeV (20 HAU/ml), EMCV (MOI = 1), NDV (MOI = 1), or HSV-1 (MOI = 1) or transfected with poly I:C H (1 μg/ml), poly dA:dT (1 μg/ml), and ISD (2 μg/ml) for 12 h before the harvest. The uninfected or untransfected cells were used as the control (Mock). The mRNA levels of *tIFNB1* and viral RNA (SeV, EMCV, NDV, and HSV-1) were measured by RT-qPCR with normalization to β-actin (right). **(C)** Overexpression of tOASL1 activated the IFN-β-Luc reporter in a dose-dependent manner in TSPRCs. The procedure was the same as in (A), except for using an increased amount (16, 80, and 400 ng) of tOASL1 expression vector (with empty vector to reach a total amount of 400 ng). **(D)** tOASL1 overexpression activated the ISRE-Luc and NF-κB-Luc reporters in TSPRCs upon NDV infection. The procedure was the same as in (A). **(E)** tOASL1 overexpression upregulated *tIFNB1*, *tISG54*, *tISG56*, and *tMx1* mRNA levels in TSPRCs upon NDV infection. The procedure was similar to (B). **(F)** Overexpression of tOASL1 enhanced the phosphorylation of IRF3, TBK1, p65, IKKα/β, and IκBα. TSPRCs ( $4 \times 10^5$ ) were transfected with the indicated expression vector for 36 h and then were infected with or without NDV (MOI = 1) for the indicated times before the harvest. tMAVS was used as a positive control in (A), (B), (D), and (E). The experiments for (A)–(F) were independently repeated three times with similar results, and the shown results were a representative experiment. Values were presented as mean  $\pm$  SD ( $n = 3$  independent experiments). \* $p < 0.05$ , \*\* $p < 0.01$ , \*\*\* $p < 0.001$ , two-tailed unpaired Student *t* test.

impaired the activation of IFN-β, ISRE, and NF-κB promoter reporters (Fig. 2B) and significantly reduced mRNA levels of *tIFNB1* and downstream ISGs (Fig. 2C). In line with this observation, tOASL1 knockdown distinctly suppressed the phosphorylation of TBK1, IRF3, p65, IKKα/β, and IκBα induced by NDV infection (Fig. 2D).

We generated tOASL1-deficient TSR6 cells (tOASL1-KO) using the CRISPR/Cas9-mediated genome editing method (Fig. 2E) to further investigate the role of endogenous tOASL1 in antiviral immune response. The replication of VSV (tagged by GFP; VSV-GFP) was significantly enhanced in tOASL1-KO cells in comparison with the wild-type (WT) TSR6 cells (Fig. 2F, 2G). Similarly, more VSV plaques (Fig. 2H, 2I) were found in tOASL1-KO cells relative to the WT cells. All these data suggested

that endogenous tOASL1 was critically involved in antiviral immune responses by positively modulating type I IFN signaling.

#### *tOASL1 promoted RNA virus-triggered IFN signaling mediated by tMDA5 and tMAVS*

We next investigated the potential mechanism by which tOASL1 enhanced RNA virus-induced type I IFN signaling pathway. TSPRCs were cotransfected with expression vectors for tMDA5, tMAVS, and tTBK1, together with tOASL1 expression vector. We found that tOASL1 overexpression enhanced the reporter activities of the IFN-β-Luc, ISRE-Luc, and NF-κB-Luc induced by tMDA5 and tMAVS, but not TBK1, in a dose-dependent manner (Fig. 3A). This result suggested that tMDA5 and tMAVS may be involved in tOASL1-regulated innate immune pathway. We further

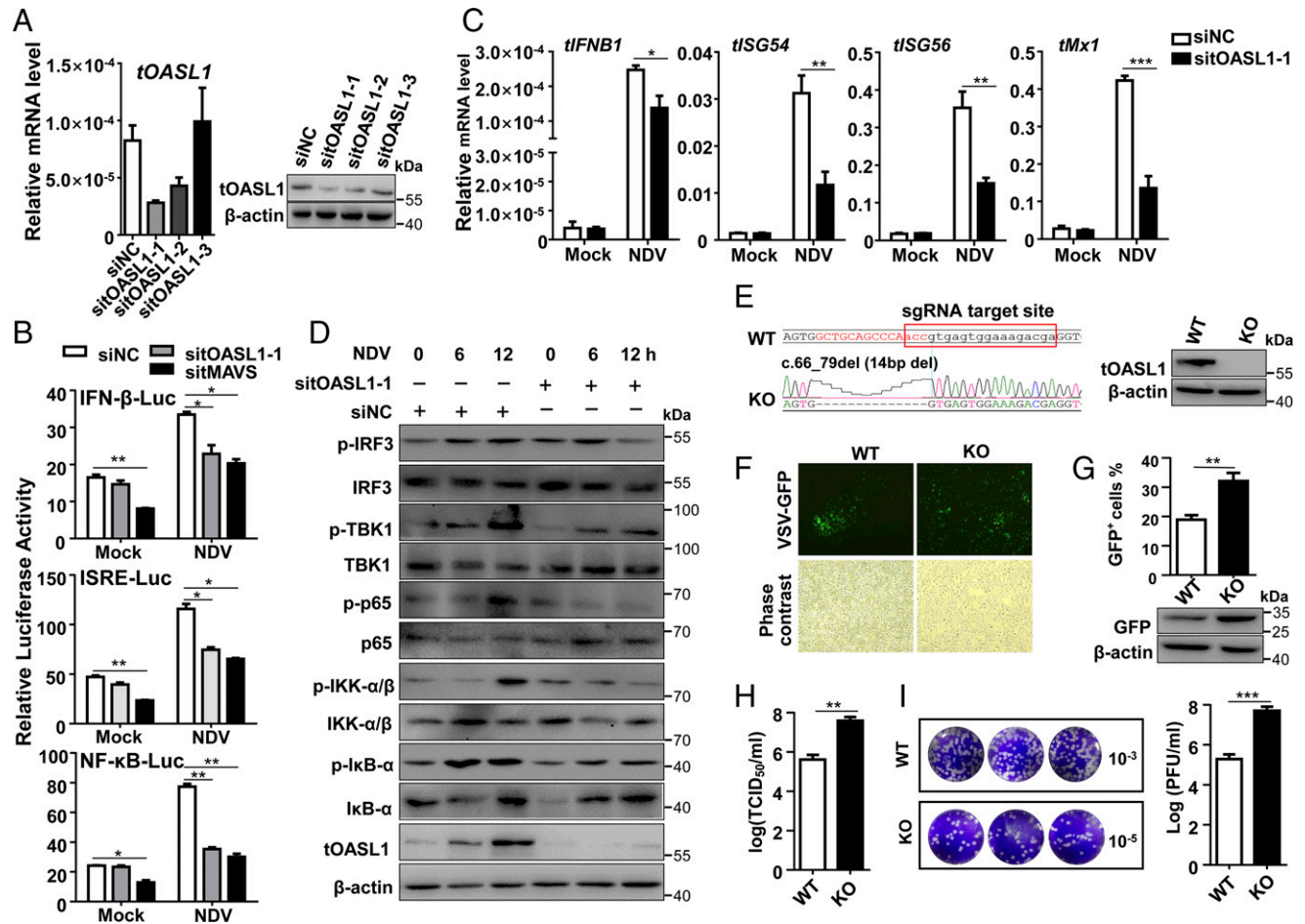


**FIGURE 2.** Knockdown or deficiency of tOASL1 impaired the antiviral responses upon RNA virus infection. **(A)** Knockdown efficiency of siRNAs targeting endogenous *tOASL1* in TSPRCs. Cells ( $1 \times 10^5$ ) were transfected with the siRNA negative control (siNC, 50 nM) or the respective siRNAs targeting to different *tOASL1* region (50 nM) for 36 h. The mRNA and protein levels of endogenous tOASL1 were measured by RT-qPCR (left) and immunoblotting analysis (right). **(B)** Knockdown of tOASL1 inhibited the activation of IFN- $\beta$ -Luc, ISRE-Luc, and NF- $\kappa$ B-Luc reporters upon NDV infection. TSPRCs ( $1 \times 10^5$ ) were cotransfected with the indicated reporter vector (100 ng), TK (10 ng), and siRNA (siNC, sitOASL1-1, and sitMAVS, each 50 nM) for 24 h, followed by NDV infection (MOI = 1) or without infection (Mock) for 12 h before the harvest for the luciferase assay. **(C)** tOASL1 knockdown significantly inhibited the mRNA expression of *tIFN $\beta$ 1* and downstream antiviral genes in TSPRCs. The procedures for siRNA transfection (36 h) and NDV infection (12 h) were the same as in (B). **(D)** tOASL1 knockdown decreased the phosphorylation of IRF3, TBK1, p65, IKK $\alpha/\beta$ , and I $\kappa$ B $\alpha$  in TSPRCs infected with NDV. **(E)** KO of the *tOASL1* gene in tree shrew renal cell line TSR6 using CRISPR/Cas9. Left, Sequencing chromatographs showing the mutation in tOASL1-KO cells. Right, The tOASL1 protein expression was found in WT cells but not in KO cells. **(F and G)** tOASL1 deficiency promoted VSV replication in TSR6 cells. Cells ( $2 \times 10^5$ ) were infected with VSV (MOI = 0.1) for 12 h (F), and the percentage of 10,000 cells expressing GFP (GFP<sup>+</sup> cells) was quantified by flow cytometry (upper) or immunoblotting (lower) for GFP expression (G). **(H and I)** The viral titers in the supernatant of VSV-infected TSR6 cells were analyzed by standard median tissue culture infective dose (TCID<sub>50</sub>) (H) and plaque assay (I). All data were representative of three independent experiments with similar results. Data were presented as mean  $\pm$  SD. \* $p < 0.05$ , \*\* $p < 0.01$ , \*\*\* $p < 0.001$ , two-tailed unpaired Student *t* test.

investigated whether tMDA5 and tMAVS mediated the tOASL1-regulated antiviral immunity. Coexpression of tOASL1 and tMDA5 or tOASL1 and tMAVS significantly upregulated the transcription of *tIFN $\beta$ 1* in TSPRCs upon NDV infection (Fig. 3B, 3C). Overexpression of all three proteins had an even stronger induction effect on *tIFN $\beta$ 1* mRNA level (Fig. 3D). In contrast, knockdown of tMDA5 or tMAVS impaired the induction of the IFN signaling in TSPRCs overexpressing tOASL1 (Fig. 3E). Taken together, these results indicated that tMDA5 and tMAVS were involved in tOASL1-regulated antiviral response.

#### tOASL1 interacted with tMDA5 and tMAVS

We next sought to determine whether tOASL1 could physically interact with tMDA5 and tMAVS. A coimmunoprecipitation assay showed that overexpressed tOASL1 interacted with tMDA5 (Fig. 3F) and tMAVS (Fig. 3G), but not *Tupaia* LGP2 (Supplemental Fig. 1A), in 293T cells. The interactions between tOASL1 and tMDA5 or tMAVS could be

confirmed by reciprocal coimmunoprecipitation assay (Fig. 3H). Furthermore, we observed that tOASL1 bound to tMDA5 and tMAVS in TSPRCs with or without NDV infection (Fig. 3I). The overexpressed tOASL1 protein was colocalized with tMDA5 (Supplemental Fig. 1B) and tMAVS (Supplemental Fig. 1C) in TSPRCs, and this colocalization pattern was not affected by NDV infection. Intriguingly, staining for exogenous tOASL1 showed that this protein could (partially) colocalize with mitochondria in TSPRCs with or without NDV infection (Fig. 3J). Whether the colocalization of tOASL1 to mitochondria was mediated by tMAVS, which is a protein located on the outer mitochondrial membrane, remained to be determined. We failed to detect the endogenous tOASL1 because of the lack of proper Ab.

#### tOASL1 interacted with tMDA5 and tMAVS via its OAS and UBL domains

To map the tOASL1 domains that interacted with tMDA5 and tMAVS, we generated a series of truncated mutants of tOASL1,

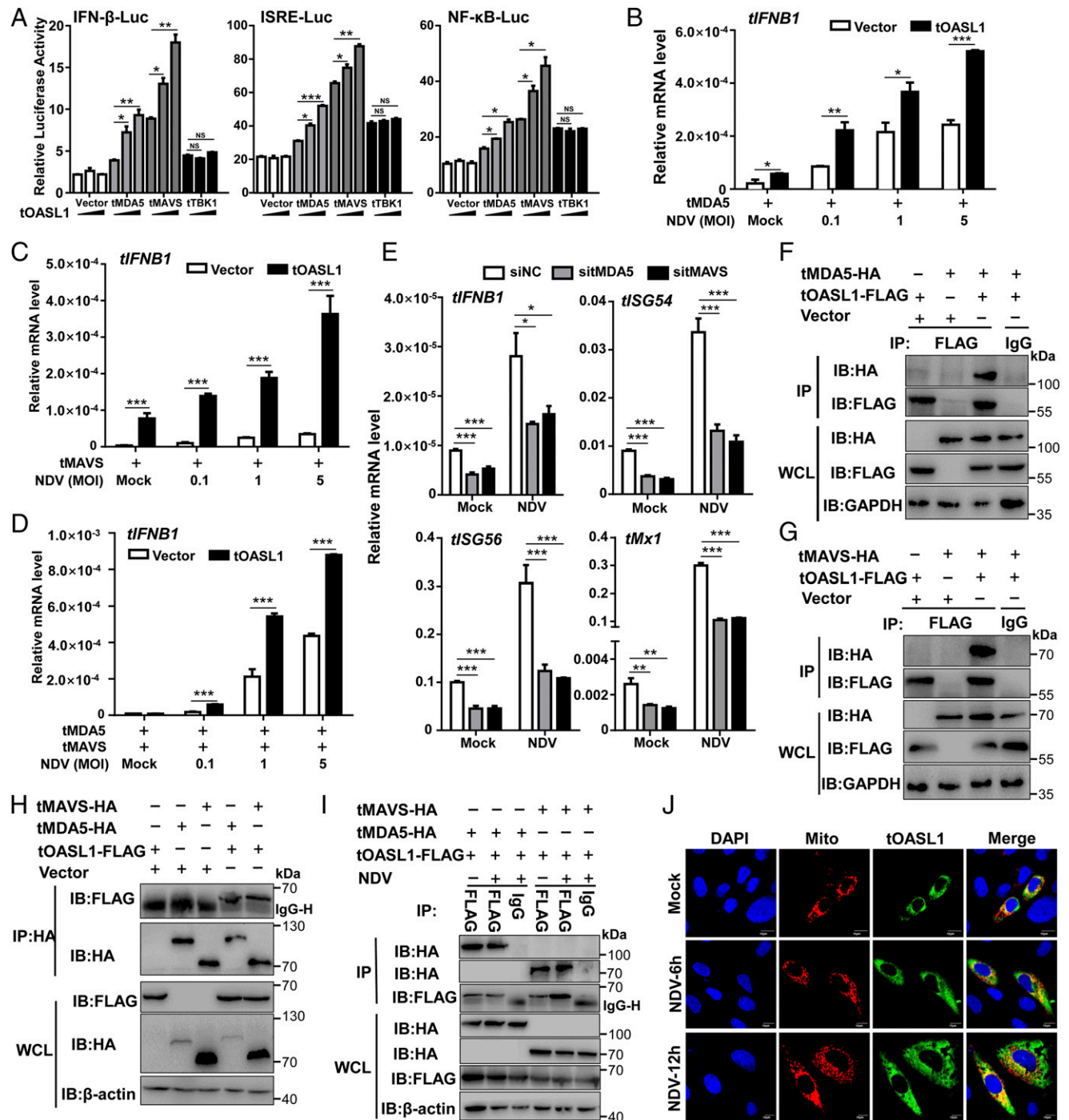


**FIGURE 3.** The regulatory effect of tOASL1 on the type I IFN signaling was mediated by tMDA5 and tMAVS. **(A)** Activation of IFN- $\beta$ -Luc, ISRE-Luc, or NF- $\kappa$ B-Luc reporter activities by coexpression of the indicated protein (tMDA5, tMAVS, and tTBK1) and different dosage of tOASL1 in TSPRCs. The procedure is similar to Fig. 1C, except for using an increased amount (80 and 400 ng) of tOASL1 expression vector (with empty vector to reach a total amount of 400 ng). **(B)** and **(C)** tOASL1 overexpression enhanced the **(B)** tMDA5- or **(C)** tMAVS-triggered IFN signaling. **(D)** tOASL1 overexpression enhanced the tMDA5 and tMAVS-triggered IFN signaling. The procedure in **(B)–(D)** was similar to Fig. 1B. **(E)** Knockdown of tMDA5 or tMAVS impaired the induction of the IFN signaling in TSPRCs overexpressing tOASL1. **(F)** and **(G)** tOASL1 interacted with tMDA5 and tMAVS. HEK293T cells ( $1 \times 10^7$ ) were cotransfected with tOASL1-FLAG and tMDA5-HA (**F**) or tOASL1-FLAG and tMAVS-HA (**G**) (each 5  $\mu$ g) for 48 h before the harvest for immunoprecipitation analysis. IgG was used as a control. **(H)** Reciprocal coimmunoprecipitation assay of **(F)** and **(G)** in HEK293T cells. IgG-H-IgG H chain. **(I)** tOASL1 interacted with tMDA5 and tMAVS in TSPRCs. The procedure was the same as in **(F)** and **(G)**. Cells were left untreated or infected with NDV (MOI = 1) for 12 h before the harvest. **(J)** Colocalization of tOASL1 with mitochondria in TSPRCs with or without NDV infection. Cells ( $1 \times 10^4$ ) were cotransfected with expression vector for tOASL1-FLAG (500 ng) and pDsRed-Mito (concentration ratio 10:1) for 36 h, followed by infection with or without NDV (MOI = 1) at the indicated times. tOASL1 was immunostained by using anti-FLAG (green), and mitochondria were directly imaged by confocal microscopy (red). Nuclei were stained with blue staining (DAPI). Scale bar, 10  $\mu$ m. All data shown were representative of three independent experiments with similar results. Values were presented as mean  $\pm$  SD. \* $p$  < 0.05, \*\* $p$  < 0.01, \*\*\* $p$  < 0.001, two-tailed unpaired Student  $t$  test. IB, immunoblot; IP, immunoprecipitation; WCL, whole cell lysates.

tMDA5, and tMAVS (Fig. 4, upper panel). Coimmunoprecipitation experiments showed that the OAS domain of tOASL1 (tOASL1-OAS) could bind to tMDA5, whereas the remaining UBL domain of tOASL1 (tOASL1-UBL) bound to tMAVS (Fig. 4A). We further mapped the tMDA5 and tMAVS domains that were required for their interaction with tOASL1, respectively. We found the CTD of tMDA5 (tMDA5-CTD) and the CARD of tMAVS (tMAVS-CARD) could interact with tOASL1, respectively. The other domains of tMDA5 and tMAVS did not bind to tOASL1 (Fig. 4B, 4C). All these results suggested that tOASL1 interacted with tMDA5 through the binding of tOASL1-OAS to tMDA5-CTD, whereas tOASL1 interacted with tMAVS through the binding of tOASL1-UBL to tMAVS-CARD.

*tOASL1 facilitated recruitment of tMDA5 to tMAVS*

As tOASL1 interacted with tMDA5 and tMAVS using different domains, we tested whether both tOASL1 domains were essential for initiating the type I IFN signaling. We found that only full-length tOASL1 (tOASL1-WT) potentiated the transcription of *tIFNB1*, *tISG54*, *tISG56*, and *tMx1* induced by NDV infection, whereas the two tOASL1 domains did not affect the induced expression of these genes (Fig. 5A). The *tIFNB1* mRNA level was significantly decreased in tOASL1-KO cells in comparison with WT TSR6 cells upon NDV infection (Fig. 5B). Introduction of tOASL1-WT, but not mutants tOASL1-OAS and tOASL1-UBL, back into tOASL1-KO cells showed that only tOASL1-WT could upregulate the transcription of *tIFNB1* (Fig. 5B). In addition, we observed a marked reduction of *tIFNB1* mRNA level in tOASL1-KO cells transfected with tMDA5, but not tMAVS (Supplemental Fig. 1D). All these results indicated that only the full-length tOASL1 was responsible for enhancing type I IFN signaling. We speculated that a combination of tOASL1, tMDA5, and tMAVS as a probable signalosome complex would play the role, although we failed to obtain direct evidence for the proposed complex (data not shown).

Upon binding to viral RNA, MDA5 was recruited to MAVS, leading to the activation of type I IFN signaling (6, 40). We investigated whether tOASL1 could facilitate the recruitment of

tMDA5 to tMAVS. Coimmunoprecipitation assay indicated that tOASL1 enhanced tMDA5 and tMAVS interaction in 293T cells (Fig. 5C). Similarly, overexpressing tOASL1 in TSPRCs could enhance the interaction of overexpressed tMDA5 and tMAVS, irrespective of NDV infection (Fig. 5D). Consistently, tOASL1 KO dramatically impaired the interaction between tMDA5 and tMAVS (Fig. 5E). We performed similar experiments to discern the potential interaction of tOASL1 with human RLRs. We observed that tOASL1 had no interaction with human MDA5 (hMDA5), human MAVS (hMAVS), and human RIG-I in 293T cells (Supplemental Fig. 1E), suggesting a potential species specificity. In addition, tOASL1 overexpression had no obvious effect on the interaction between hMDA5 and hMAVS in TSPRCs, irrespective of NDV infection (Supplemental Fig. 1F). Consistently, overexpressing tOASL1 in HeLa cells also facilitated the recruitment of tMDA5 to tMAVS but not hMDA5 to hMAVS (Supplemental Fig. 1G).

Because the interaction between MDA5 and MAVS is critical for initiating the type I IFN signaling (40, 41) and tOASL1 can colocalize with mitochondria (Fig. 3J), we asked whether tOASL1 can facilitate the recruitment of tMDA5 to mitochondria upon NDV infection. We found that tOASL1 overexpression increased endogenous tMDA5 levels in mitochondria in TSPRCs infected with NDV (Fig. 5F), whereas the level of tMDA5 in the crude mitochondria was substantially decreased when tOASL1 was absent (Fig. 5G). Together, our results indicated that tOASL1 was required for enhanced interaction between tMDA5 and tMAVS, and tOASL1 promoted the recruitment of tMDA5 to tMAVS on mitochondria (Fig. 5H).

**Discussion**

During viral infection, RIG-I and MDA5 are well-known nucleic acid sensors to bind viral dsRNAs and are recruited to the adaptor protein MAVS, which acts as a central scaffold for a virus-induced complex assembly (6, 8). This process is critical for triggering distinct signaling pathways and the induction of type I IFNs. Although ATP-dependent conformational change allows CARDS of RIG-I and MDA5 to interact with MAVS and leads to the

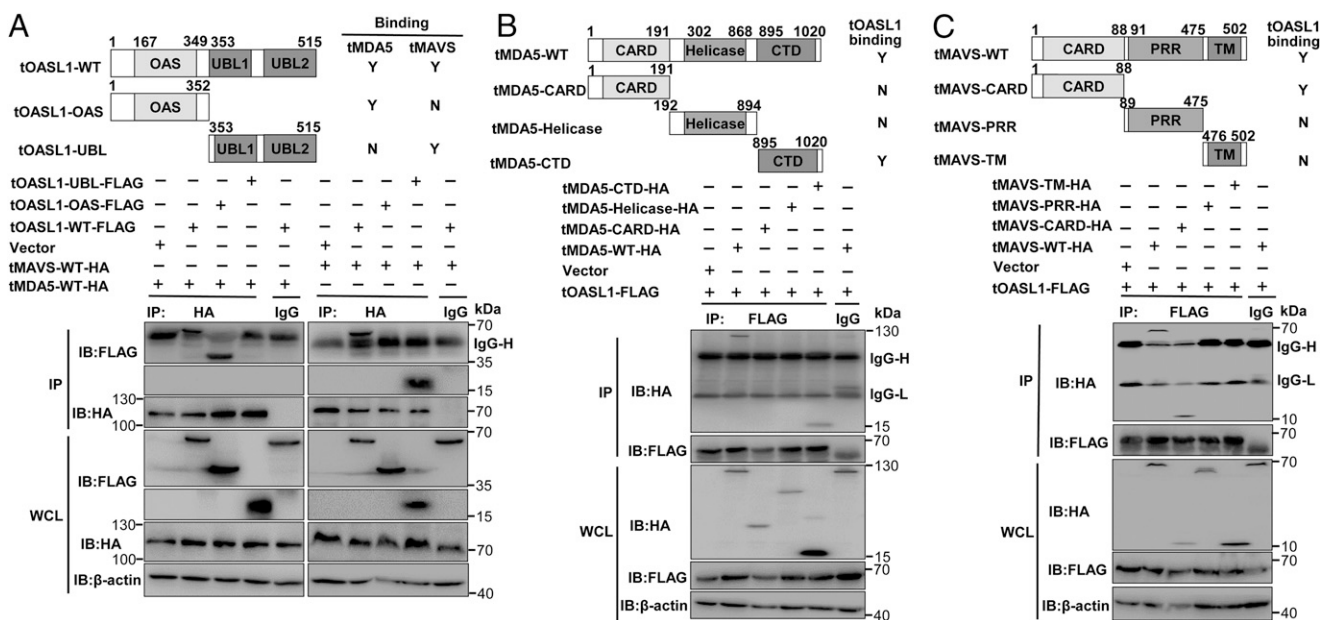


**FIGURE 4.** Domain mapping of tOASL1 for interaction with tMDA5 and tMAVS. (A–C) HEK293T cells ( $1 \times 10^7$ ) were cotransfected with the indicated expression vectors for tOASL1, tMDA5, tMAVS, and/or the related domains (each 5  $\mu$ g). Cells were harvested at 48 h, and immunoprecipitation assays were performed following the procedure in Fig. 3F. IgG-L–IgG L chain.

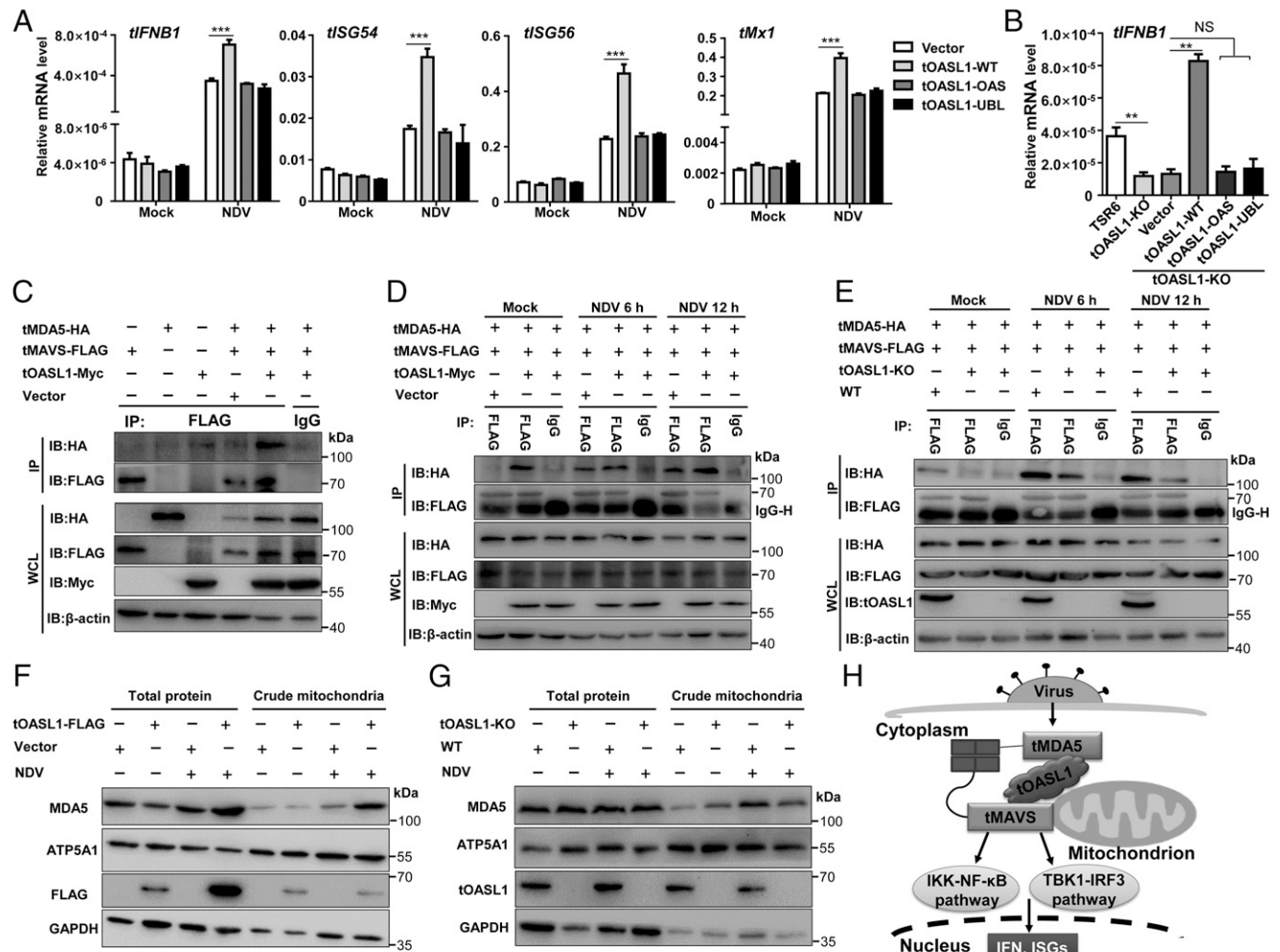


**FIGURE 5.** tOASL1 potentiated the IFN signaling by recruiting tMDA5 to tMAVS. **(A)** Overexpression of tOASL1, but not its domains, increased the mRNA levels of *tIFNB1* and downstream ISGs in TSPRCs with NDV infection. The procedure was the same as in Fig. 1B. **(B)** Overexpression of tOASL1 in tOASL1-KO cells could rescue NDV-induced *tIFNB1* expression. Cells ( $1 \times 10^5$ ) were transfected with tOASL1-WT or its mutants (tOASL1-OAS and tOASL1-UBL) (each 500 ng) for 36 h, followed by infection with NDV (MOI = 1) for 12 h before the harvest for RT-qPCR. **(C)** Overexpression of tOASL1 promoted the interaction between tMDA5 and tMAVS in HEK293T cells. Cells ( $1 \times 10^7$ ) were transfected with Myc-tagged tOASL1 (5  $\mu$ g) or tMAVS-FLAG (5  $\mu$ g) and tMDA5-HA (5  $\mu$ g) for 48 h before the harvest for immunoprecipitation assays. **(D)** Overexpression of tOASL1 enhanced the tMDA5 and tMAVS interaction in TSPRCs infected with or without NDV infection. The immunoprecipitation procedure was the similar as in (C). **(E)** tOASL1 deficiency decreased the tMDA5 and tMAVS interaction in TSR6 cells. tOASL1-KO or TSR6-WT (WT) cells ( $1 \times 10^7$ ) were transfected with tMDA5-HA (5  $\mu$ g) and tMAVS-FLAG (5  $\mu$ g) for 36 h, followed by infection with or without NDV (MOI = 1) for 12 h before the immunoprecipitation assays. **(F)** Overexpression of tOASL1 increased the recruitment of tMDA5 to mitochondria in TSR6 cells with NDV infection. TSR6 cells ( $1 \times 10^7$ ) were transfected with control vector (Vector) or tOASL1-FLAG (each 5  $\mu$ g) for 36 h. Cells then were left untreated or infected with NDV (MOI = 1) for 12 h before the harvest for the isolation of crude mitochondria and for collecting whole cell lysate (total protein). **(G)** KO of tOASL1 decreased the recruitment of tMDA5 to mitochondria in TSR6 cells with NDV infection. The procedure was similar to (F). **(H)** A working model illustrating the role of tOASL1 in potentiating type I IFN signaling upon RNA virus infection via interaction of tMDA5 and tMAVS. All data were representative of three independent experiments showing similar results. Bars represent mean  $\pm$  SD. \*\* $p < 0.01$ , \*\*\* $p < 0.001$ , two-tailed unpaired Student *t* test.

formation of the MAVS signalosome (10), how this process is mediated remains unclear. Several lines of evidence suggest that some host proteins are critical for controlling the association of RIG-I or MDA5 with the adaptor MAVS, such as ECSIT signaling integrator (ECSIT) (42), Zyxin (43), NLR family pyrin domain containing 12 (44), and the most recently reported nucleotide binding oligomerization domain containing 1 (45). In this study, we found that tOASL1, a member of 2',5'-OAS family proteins, potentiated RNA virus-induced signaling cascade in the Chinese tree shrew by recruiting tMDA5 to tMAVS. This finding provided another line of evidence for the complexity of assembling the MAVS signalosome, especially considering the fact that RIG-I was naturally lost in the Chinese tree shrew (24, 34).

The OASL belonged to the OAS family proteins characterized by its N-terminal OASL domain but was devoid of the enzymatic activity to activate the OAS/RNase L pathway (19). In our previous study, we found that the cDNA of tOASL1 was 2176 bp in length and encoded a polypeptide of 514 aa, which shared 75.4% residue identity to human ortholog of OASL. tOASL1 contained a typical N-terminal OAS domain and two tandem ubiquitin-like domains at the C-terminal. Phylogenetic analyses revealed that tOASL1 was first clustered with the corresponding orthologs of primates, indicating that tOASL1 was relatively conserved in the Chinese tree shrew (23). In addition, we found that the mRNA levels of tOASL1 and the other three tOASs (tOAS1, tOAS2, and tOASL2) were significantly increased in cells upon DNA virus (HSV-1) or RNA virus (SeV, NDV, and VSV) infection compared with uninfected

TSPRCs (23). These available results indicated that tOASs were ISGs. Several studies had reported that OASL played an essential role in modulating virus-induced type I IFN signaling pathway (20–22, 46), albeit the role of OASL in human (20, 21) was different from that of mouse (22), indicating a potential species-specific pattern. Similar to human OASL (hOASL) (20) and porcine OASL (46), the tOASL1 was actively involved in RNA virus-induced IFN induction pathway and acted as a positive regulator. However, tOASL1 differed from hOASL in several aspects. First, although hOASL and tOASL1 commonly promoted RNA virus-induced IFN induction, tOASL1 had no effect on IFN production upon DNA virus (Fig. 1A, 1B), whereas hOASL had an inhibitory effect (21). Note that mouse *Oasl1* had an inhibitory effect on both RNA virus- and DNA virus-induced IFN inductions (22). The exact reason for this species-specific role remained unknown, but this offered a good opportunity for us to learn the evolutionary complexity and compensation of the immune system. Second, different from hOASL, which interacted and colocalized with RIG-I to mediate the downstream effect (20), tOASL1 interacted with tMDA5 and tMAVS and potentiated the tMDA5- and tMAVS-triggered IFN inductions (Fig. 3). We believe this difference was compatible with the fact that RIG-I was naturally lost, and MDA5 had a functional replacement in the Chinese tree shrew (34). Moreover, we found that tOASL1 could colocalize and interacted with MAVS. Similar to the mitochondrion-localized ZNFX1 (47), no predicted mitochondrial targeting motif was found for tOASL1. The OAS domain had been reported to be associated with mitochondria (48), and the UBL domain of tOASL1 was critical for interacting with tMAVS (Fig. 4A), which might be responsible for the mitochondrial localization of tOASL1, irrespective of RNA virus infection. To our knowledge, this is the first time that OASL was found to be localized in mitochondria, which would facilitate its natural interaction with MAVS.

Another interesting observation in this study is that tOASL1 promoted the recruitment of tMDA5 to tMAVS (Fig. 5C–G, Supplemental Fig. 1G). In particular, tOASL1 interacted with tMDA5 and tMAVS using different domains, which might be helpful for forming the tOASL1–tMDA5–tMAVS complex. It is pitiful that we were unable to isolate this protein complex (presumably because of its large size) and make further characterization. Note that overexpression of tOASL1 domains, but not full-length tOASL1, could not enhance NDV-induced transcription of *tIFNB1* and downstream antiviral genes (Fig. 5A). In addition, tOASL1 deficiency dramatically impaired the interaction between tMDA5 and tMAVS (Fig. 5E). On this point, tOASL1 not only acts as a scaffold protein bridging tMDA5 and tMAVS but also works as a positive regulator of antiviral signaling to counteract RNA virus infection.

In summary, we identified tOASL1 as a positive regulator of the type I IFN induction by recruiting tMDA5 to tMAVS to counteract RNA virus infection. We further elucidated the molecular mechanism by which tOASL1 positively regulates the anti-RNA virus innate immunity. The multifaceted role of OASL illustrated a unique picture of the innate immunity in different species.

## Acknowledgments

We thank Dr. Rongcan Luo for technical assistance. We also thank Dr. Yong Wu for critical discussion and communication of unpublished results. The study was done at KIZ, CAS.

## Disclosures

The authors have no financial conflicts of interest.

## References

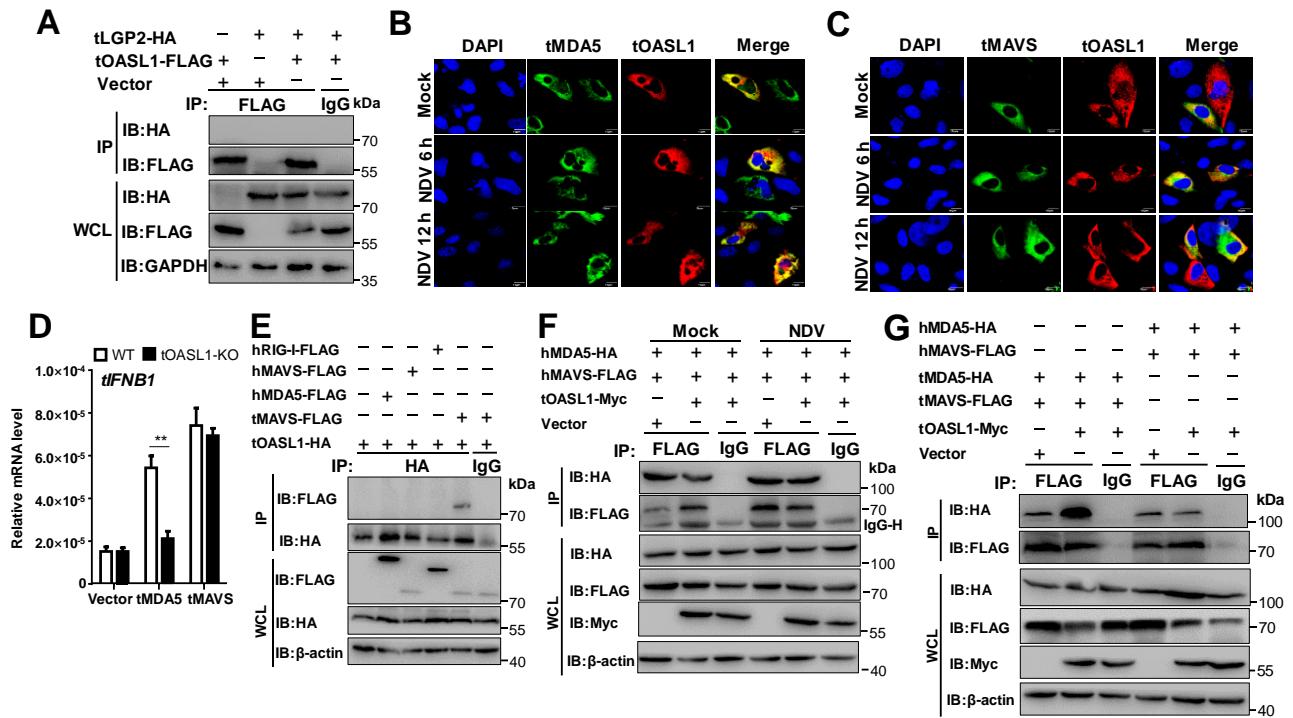
- Akira, S., S. Uematsu, and O. Takeuchi. 2006. Pathogen recognition and innate immunity. *Cell* 124: 783–801.
- Wu, J., and Z. J. Chen. 2014. Innate immune sensing and signaling of cytosolic nucleic acids. *Annu. Rev. Immunol.* 32: 461–488.
- Kato, H., O. Takeuchi, S. Sato, M. Yoneyama, M. Yamamoto, K. Matsui, S. Uematsu, A. Jung, T. Kawai, K. J. Ishii, et al. 2006. Differential roles of MDA5 and RIG-I helicases in the recognition of RNA viruses. *Nature* 441: 101–105.
- Yoneyama, M., and T. Fujita. 2009. RNA recognition and signal transduction by RIG-I-like receptors. *Immunol. Rev.* 227: 54–65.
- Seth, R. B., L. Sun, C. K. Ea, and Z. J. Chen. 2005. Identification and characterization of MAVS, a mitochondrial antiviral signaling protein that activates NF- $\kappa$ B and IRF 3. *Cell* 122: 669–682.
- Kawai, T., K. Takahashi, S. Sato, C. Coban, H. Kumar, H. Kato, K. J. Ishii, O. Takeuchi, and S. Akira. 2005. IPS-1, an adaptor triggering RIG-I- and Mda5-mediated type I interferon induction. *Nat. Immunol.* 6: 981–988.
- Meylan, E., J. Curran, K. Hofmann, D. Moradpour, M. Binder, R. Bartenschlager, and J. Tschopp. 2005. Cardif is an adaptor protein in the RIG-I antiviral pathway and is targeted by hepatitis C virus. *Nature* 437: 1167–1172.
- Xu, L. G., Y. Y. Wang, K. J. Han, L. Y. Li, Z. Zhai, and H. B. Shu. 2005. VISA is an adaptor protein required for virus-triggered IFN- $\beta$  signaling. *Mol. Cell* 19: 727–740.
- Hou, F., L. Sun, H. Zheng, B. Skaug, Q. X. Jiang, and Z. J. Chen. 2011. MAVS forms functional prion-like aggregates to activate and propagate antiviral innate immune response. [Published erratum appears in 2011 *Cell* 146: 841.] *Cell* 146: 448–461.
- Potter, J. A., R. E. Randall, and G. L. Taylor. 2008. Crystal structure of human IPS-1/MAVS/VISA/Cardif caspase activation recruitment domain. *BMC Struct. Biol.* 8: 11.
- Schneider, W. M., M. D. Chevillotte, and C. M. Rice. 2014. Interferon-stimulated genes: a complex web of host defenses. *Annu. Rev. Immunol.* 32: 513–545.
- Yoneyama, M., M. Kikuchi, K. Matsumoto, T. Imaizumi, M. Miyagishi, K. Taira, E. Foy, Y. M. Loo, M. Gale, Jr., S. Akira, et al. 2005. Shared and unique functions of the DExD/H-box helicases RIG-I, MDA5, and LGP2 in antiviral innate immunity. *J. Immunol.* 175: 2851–2858.
- Satoh, T., H. Kato, Y. Kumagai, M. Yoneyama, S. Sato, K. Matsushita, T. Tsujimura, T. Fujita, S. Akira, and O. Takeuchi. 2010. LGP2 is a positive regulator of RIG-I- and MDA5-mediated antiviral responses. *Proc. Natl. Acad. Sci. USA* 107: 1512–1517.
- Ablasser, A., and S. Hur. 2020. Regulation of cGAS- and RLR-mediated immunity to nucleic acids. *Nat. Immunol.* 21: 17–29.
- Liu, J., C. Qian, and X. Cao. 2016. Post-translational modification control of innate immunity. *Immunity* 45: 15–30.
- Eskildsen, S., J. Justesen, M. H. Schierup, and R. Hartmann. 2003. Characterization of the 2'-5'-oligoadenylate synthetase ubiquitin-like family. *Nucleic Acids Res.* 31: 3166–3173.
- Hartmann, R., J. Justesen, S. N. Sarkar, G. C. Sen, and V. C. Yee. 2003. Crystal structure of the 2'-specific and double-stranded RNA-activated interferon-induced antiviral protein 2'-5'-oligoadenylate synthetase. *Mol. Cell* 12: 1173–1185.
- Silverman, R. H. 2007. Viral encounters with 2',5'-oligoadenylate synthetase and RNase L during the interferon antiviral response. *J. Virol.* 81: 12720–12729.
- Zhu, J., A. Ghosh, and S. N. Sarkar. 2015. OASL—a new player in controlling antiviral innate immunity. *Curr. Opin. Virol.* 12: 15–19.
- Zhu, J., Y. Zhang, A. Ghosh, R. A. Cuevas, A. Forero, J. Dhar, M. S. Ibsen, J. L. Schmid-Burgk, T. Schmidt, M. K. Ganapathiraju, et al. 2014. Antiviral activity of human OASL protein is mediated by enhancing signaling of the RIG-I RNA sensor. *Immunity* 40: 936–948.
- Ghosh, A., L. Shao, P. Sampath, B. Zhao, N. V. Patel, J. Zhu, B. Behl, R. A. Parise, J. H. Beumer, R. J. O'Sullivan, et al. 2019. Oligoadenylate-synthetase-family protein OASL inhibits activity of the DNA sensor cGAS during DNA virus infection to limit interferon production. *Immunity* 50: 51–63.e5.
- Lee, M. S., B. Kim, G. T. Oh, and Y. J. Kim. 2013. OASL1 inhibits translation of the type I interferon-regulating transcription factor IRF7. [Published erratum appears in 2013 *Nat. Immunol.* 14: 355.] *Nat. Immunol.* 14: 346–355.
- Yao, Y. L., D. Yu, L. Xu, Y. Fan, Y. Wu, T. Gu, J. Chen, L. B. Lv, and Y. G. Yao. 2019. Molecular characterization of the 2',5'-oligoadenylate synthetase family in the Chinese tree shrew (*Tupaia belangeri chinensis*). *Cytokine* 114: 106–114.
- Fan, Y., Z. Y. Huang, C. C. Cao, C. S. Chen, Y. X. Chen, D. D. Fan, J. He, H. L. Hou, L. Hu, X. T. Hu, et al. 2013. Genome of the Chinese tree shrew. *Nat. Commun.* 4: 1426.
- Fan, Y., M. S. Ye, J. Y. Zhang, L. Xu, D. D. Yu, T. L. Gu, Y. L. Yao, J. Q. Chen, L. B. Lv, P. Zheng, et al. 2019. Chromosomal level assembly and population sequencing of the Chinese tree shrew genome. *Zool. Res.* 40: 506–521.
- Xu, S., X. Li, J. Yang, Z. Wang, Y. Jia, L. Han, L. Wang, and Q. Zhu. 2019. Comparative pathogenicity and transmissibility of pandemic H1N1, avian H5N1, and human H7N9 influenza viruses in tree shrews. *Front. Microbiol.* 10: 2955.
- Xiao, J., R. Liu, and C. S. Chen. 2017. Tree shrew (*Tupaia belangeri*) as a novel laboratory disease animal model. *Zool. Res.* 38: 127–137.
- Yao, Y. G. 2017. Creating animal models, why not use the Chinese tree shrew (*Tupaia belangeri chinensis*)? *Zool. Res.* 38: 118–126.
- Amako, Y., K. Tsukiyama-Kohara, A. Katsume, Y. Hirata, S. Sekiguchi, Y. Tobita, Y. Hayashi, T. Hishima, N. Funata, H. Yonekawa, and M. Kohara.

2010. Pathogenesis of hepatitis C virus infection in *Tupaia belangeri*. *J. Virol.* 84: 303–311.
30. Xu, L., D. D. Yu, Y. H. Ma, Y. L. Yao, R. H. Luo, X. L. Feng, H. R. Cai, J. B. Han, X. H. Wang, M. H. Li, et al. 2020. COVID-19-like symptoms observed in Chinese tree shrews infected with SARS-CoV-2. *Zool. Res.* 41: 517–526.
  31. Zhang, J., R. C. Luo, X. Y. Man, L. B. Lv, Y. G. Yao, and M. Zheng. 2020. The anatomy of the skin of the Chinese tree shrew is very similar to that of human skin. *Zool. Res.* 41: 208–212.
  32. Fan, Y., R. Luo, L. Y. Su, Q. Xiang, D. Yu, L. Xu, J. Q. Chen, R. Bi, D. D. Wu, P. Zheng, and Y. G. Yao. 2018. Does the genetic feature of the Chinese tree shrew (*Tupaia belangeri chinensis*) support its potential as a viable model for Alzheimer's disease research? *J. Alzheimers Dis.* 61: 1015–1028.
  33. Ni, R. J., Y. Tian, X. Y. Dai, L. S. Zhao, J. X. Wei, J. N. Zhou, X. H. Ma, and T. Li. 2020. Social avoidance behavior in male tree shrews and prosocial behavior in male mice toward unfamiliar conspecifics in the laboratory. *Zool. Res.* 41: 258–272.
  34. Xu, L., D. Yu, Y. Fan, L. Peng, Y. Wu, and Y. G. Yao. 2016. Loss of RIG-I leads to a functional replacement with MDA5 in the Chinese tree shrew. *Proc. Natl. Acad. Sci. USA* 113: 10950–10955.
  35. Xu, L., D. Yu, L. Peng, Y. Fan, J. Chen, Y. T. Zheng, C. Wang, and Y. G. Yao. 2015. Characterization of a MAVS ortholog from the Chinese tree shrew (*Tupaia belangeri chinensis*). *Dev. Comp. Immunol.* 52: 58–68.
  36. Ma, X., A. S. Wong, H. Y. Tam, S. Y. Tsui, D. L. Chung, and B. Feng. 2018. *In vivo* genome editing thrives with diversified CRISPR technologies. *Zool. Res.* 39: 58–71.
  37. Gu, T., D. Yu, Y. Li, L. Xu, Y. L. Yao, and Y. G. Yao. 2019. Establishment and characterization of an immortalized renal cell line of the Chinese tree shrew (*Tupaia belangeri chinensis*). *Appl. Microbiol. Biotechnol.* 103: 2171–2180.
  38. Xu, L., D. Yu, L. Peng, Y. Wu, Y. Fan, T. Gu, Y. L. Yao, J. Zhong, X. Chen, and Y. G. Yao. 2020. An alternative splicing of *tupaia* STING modulated anti-RNA virus responses by targeting MDA5-LGP2 and IRF3. *J. Immunol.* 204: 3191–3204.
  39. Xu, L., L. Peng, T. Gu, D. Yu, and Y. G. Yao. 2019. The 3'UTR of human MAVS mRNA contains multiple regulatory elements for the control of protein expression and subcellular localization. *Biochim. Biophys. Acta Gene Regul. Mech.* 1862: 47–57.
  40. Wu, B., and S. Hur. 2015. How RIG-I like receptors activate MAVS. *Curr. Opin. Virol.* 12: 91–98.
  41. Takeuchi, O., and S. Akira. 2008. MDA5/RIG-I and virus recognition. *Curr. Opin. Immunol.* 20: 17–22.
  42. Lei, C. Q., Y. Zhang, M. Li, L. Q. Jiang, B. Zhong, Y. H. Kim, and H. B. Shu. 2015. ECSIT bridges RIG-I-like receptors to VISA in signaling events of innate antiviral responses. *J. Innate Immun.* 7: 153–164.
  43. Kowaki, T., M. Okamoto, H. Tsukamoto, Y. Fukushima, M. Matsumoto, T. Seya, and H. Oshiumi. 2017. Zyxin stabilizes RIG-I and MAVS interactions and promotes type I interferon response. *Sci. Rep.* 7: 11905.
  44. Chen, S.-T., L. Chen, D. S.-C. Lin, S.-Y. Chen, Y.-P. Tsao, H. Guo, F.-J. Li, W.-T. Tseng, J. W. Tam, C.-W. Chao, et al. 2019. NLRP12 regulates anti-viral RIG-I activation via interaction with TRIM25. *Cell Host Microbe* 25: 602–616.e7.
  45. Wu, X. M., J. Zhang, P. W. Li, Y. W. Hu, L. Cao, S. Ouyang, Y. H. Bi, P. Nie, and M. X. Chang. 2020. NOD1 promotes antiviral signaling by binding viral RNA and regulating the interaction of MDA5 and MAVS. *J. Immunol.* 204: 2216–2231.
  46. Li, L.-F., J. Yu, Y. Zhang, Q. Yang, Y. Li, L. Zhang, J. Wang, S. Li, Y. Luo, Y. Sun, and H. J. Qiu. 2017. Interferon-inducible oligoadenylate synthetase-like protein acts as an antiviral effector against classical swine fever virus via the MDA5-mediated type I interferon-signaling pathway. *J. Virol.* 91: e01514-16.
  47. Wang, Y., S. Yuan, X. Jia, Y. Ge, T. Ling, M. Nie, X. Lan, S. Chen, and A. Xu. 2019. Mitochondria-localised ZNFX1 functions as a dsRNA sensor to initiate antiviral responses through MAVS. *Nat. Cell Biol.* 21: 1346–1356.
  48. Kjøer, K. H., J. Pahuš, M. F. Hansen, J. B. Poulsen, E. I. Christensen, J. Justesen, and P. M. Martensen. 2014. Mitochondrial localization of the OAS1 p46 isoform associated with a common single nucleotide polymorphism. *BMC Cell Biol.* 15: 33.

Table S1. Primers and vectors used in this study.

| Primer                 | Sequence (5'-3')                       | Restriction endonuclease <sup>a</sup> | Application and vector   |
|------------------------|--|---------------------------------------|--|
| tIFNB1-F               | ACCACTTGGAACCATGC                      | -                                     | Analytical RT-qPCR for <i>tIFNB1</i>                                 |
| tIFNB1-R               | TTTCCACTCGGACTATCG                     |                                       |  |
| tISG54-F               | CTATCTGTATTGCCGTATTGG                  | -                                     | Analytical RT-qPCR for <i>tISG54</i>                                 |
| tISG54-R               | CTTCTGTCCTCTCCTCTG                     |                                       |  |
| tMx1-F                 | GAAGACATTAGACTAGAACAAGAA               | -                                     | Analytical RT-qPCR for <i>tMx1</i>                                   |
| tMx1-R                 | TCCTGGCAGTAGACAATC                     |                                       |  |
| tISG56-F               | AGAGCAGCCGTCATTTAC                     | -                                     | Analytical RT-qPCR for <i>tISG56</i>                                 |
| tISG56-R               | CAGGGCTTCCTTTAGTTC                     |                                       |  |
| tOASL1-BspE I-F        | ACT <u>TCGGA</u> ATGGCACTGGCCGAGGAGC   | <i>BspE I</i>                         | PCR for constructing tOASL1-Myc vector using pCS-myc-N vector        |
| tOASL1-Sac I-R         | CC <u>GAGCTC</u> CTACCTGGATGGAAACAGA   | <i>Sac I</i>                          |  |
| tOASL1-OAS-NotI-F      | TT <u>GCGGCCGC</u> ATGGCACTGGCCGAGGAGC | <i>Not I</i>                          | PCR for constructing tOASL1-OAS-FLAG vector using pCMV-3Tag-8 vector |
| tOASL1-OAS-EcoRV-R     | TT <u>GATATC</u> GTCTCGGGCTCTCTGCACA   | <i>EcoR V</i>                         |  |
| tOASL1-UBL-NotI-F      | TT <u>GCGGCCGC</u> ATGATCCAGGTGACAGTGG | <i>Not I</i>                          | PCR for constructing tOASL1-UBL-FLAG vector using pCMV-3Tag-8 vector |
| tOASL1-UBL-XhoI-R      | CC <u>CTCGAG</u> CCTGGATGGAAACAGAGGC   | <i>Xho I</i>                          |  |
| tMDA5-CARD-EcoRI-F     | CG <u>GAATTCAA</u> ATGTGCAATGGGCATTCTT | <i>EcoR I</i>                         | PCR for constructing HA-tMDA5-CARD vector using pCMV-HA vector       |
| tMDA5-CARD-XhoI-R      | CC <u>CTCGAG</u> CTAATCGTTTCCTGTTTTT   | <i>Xho I</i>                          |  |
| tMDA5-Helicase-EcoRI-F | CG <u>GAATTCAA</u> CTACAGCTCAGGCCTTACC | <i>EcoR I</i>                         | PCR for constructing HA-tMDA5-Helicase vector using pCMV-HA vector   |
| tMDA5-Helicase-XhoI-R  | CC <u>CTCGAG</u> CTAAATCTTATGAGCATAAC  | <i>Xho I</i>                          |  |
| tMDA5-CTD-EcoRI-F      | CG <u>GAATTCAA</u> CCATCATTAACTTTGTC   | <i>EcoR I</i>                         | PCR for constructing HA-tMDA5-CTD vector using pCMV-HA vector        |
| tMDA5-CTD-XhoI-R       | CC <u>CTCGAG</u> CTAATCCTCATCACTAAAC   | <i>Xho I</i>                          |  |
| tMAVS-CARD-XhoI-F      | CC <u>CTCGAG</u> AAATGTCATTTGCCGAGAACA | <i>Xho I</i>                          | PCR for constructing HA-tMAVS-CARD vector using pCMV-HA vector       |
| tMAVS-CARD-NotI-R      | TT <u>GCGGCCGC</u> ACGGGTCCTCCTCGGGC   | <i>Not I</i>                          |  |
| tMAVS-PRR-XhoI-F       | CC <u>CTCGAG</u> AAATGGTCTACCAGACCTACC | <i>Xho I</i>                          | PCR for constructing HA-tMAVS-PRR vector using pCMV-HA vector        |
| tMAVS-PRR-NotI-R       | TT <u>GCGGCCGC</u> AACCCTGACACACGGCTCC | <i>Not I</i>                          |  |
| tMAVS-TM-XhoI-F        | CC <u>CTCGAG</u> AAATGTCATGGCTTGGGGTGG | <i>Xho I</i>                          | PCR for constructing HA-tMAVS-TM vector using pCMV-HA vector         |
| tMAVS-TM-NotI-R        | TT <u>GCGGCCGC</u> CTACTGGAGTGGGCGCCGC | <i>Not I</i>                          |  |
| tTBK1-SacI-F           | CG <u>GAGCTC</u> ATGCAGAGCACTTCCAATCA  | <i>Sac I</i>                          | PCR for constructing tTBK1-FLAG vector using pCMV-3Tag-8 vector      |
| tTBK1-XhoI-R           | CCG <u>CTCGAG</u> AAGACAGTCCACGTTGCGAA | <i>Xho I</i>                          |  |

<sup>a</sup> Restriction endonuclease sites introduced by PCR are underlined. RT-qPCR, quantitative real-time PCR.



**Supplementary Figure 1. tOASL1 did not interact with tLGP2, and co-localized with tMDA5 and tMAVS.**

(A) No interaction of tOASL1 and tLGP2 in HEK293T cells. The procedure was same to Figure 3F.

(B-C) tOASL1 co-localized with tMDA5 and tMAVS in TSPRCs with or without NDV infection.

Cells ( $1 \times 10^4$ ) were co-transfected with expression vector for tOASL1-FLAG (300 ng) and tMDA5-HA (300 ng) or tMAVS-EGFP (300 ng) for 36 h, followed by infection with or without NDV (MOI=1) at the indicated times. tOASL1-FLAG and tMDA5-HA were immunostained by using anti-FLAG (red) and anti-HA (green) antibody, respectively. Nuclei were stained with blue staining (DAPI). Scale bar, 10  $\mu$ m.

(D) Knockout of tOASL1 impaired tMDA5-triggered *tIFNB1* expression. tOASL1-KO cells ( $1 \times 10^5$ ) were transfected with tMDA5, tMAVS or vector (each 500 ng) for 48h before the harvest for RT-qPCR.

(E) tOASL1 did not interact with hMDA5, hMAVS and hRIG-I in HEK293T cells. The procedure was same to Figure 3F.

(F) tOASL1 had no effect on the interaction between hMDA5 and hMAVS in TSPRCs. The procedure was same to Figure 5D.

(G) tOASL1 promoted the recruitment of tMDA5 to tMAVS in HeLa cells with NDV infection. The procedure was same to Figure 5D.

Shown were representative results from three independent experiments.